CAN THE STREAMING INSTABILITY FORM THE FIRST PLANETESIMALS IN GLOBALLY TURBULENT PROTOPLANETARY DISKS? P. R. Estrada[1] and O. M. Umurhan[1,2], [1]NASA Ames Research Center (MS 245-3, Moffett Field, CA 94035, Paul.R.Estrada@nasa.gov) [2]Carl Sagan Center, SETI Institute (339 N. Bernardo Ave, Suite 200, Mountain View, CA 94043, oumurhan@seti.org).

Introduction: Understanding the formation of the first planetesimals remains key to deciphering the history of planet formation within our own solar system and beyond. Evidence from the vast meteorite record [e.g., 1] as well as observations [e.g., 2] strongly suggest that the first planetesimals, and perhaps giant planet core accretion occurred well within the first million years of disk evolution. Moreover, chemical and lithological mixing as well as observations of line-broadening in protoplanetary disks (PPDs) [e.g., 3-6] suggest that the solar system nebula in this epoch was weakly-to-moderately turbulent in the regions where particle growth is of the greatest interest [7-8]. It is a well-known though that global hydrodynamic turbulence complicates particle growth due to a slew of barriers that can slow or even stall particle or aggregate growth at pebble sizes (with corresponding small particle Stokes numbers St) that can lead to loss to the central star via radial drift before planetesimals can ever form [9,10], requiring that some other mechanism come into play that collects growth-frustrated pebbles into gravitationally bound multi-km bodies – objects that are "born big" [11].

The current leading candidate for such a "leap-frog" mechanism is the so-called Streaming Instability (SI), a gas-drag mediated momentum exchange resonance in which the relative velocity between the particle component and a rotating gaseous fluid can lead to high densities in the particle field [12], which has been invoked in a number of recent PPD models that include a turbulent intensity α [e.g., 13-14] as the defacto mechanism for planetesimal formation if conditions for the SI (depending on particle St and the solids-to-gas mass ratio) are satisfied. However, these previous works use conditions established from occurrence studies for the onset of SI in laminar disks [15-17] in which the only source of turbulence is that self-generated by the settling particle layer, and not externally driven global turbulence. Recent analytical theories of the SI subject to global turbulence predict much more stringent conditions for the effectiveness of the SI than the laminar case [18-19]. Thus, whether the efficient operation of the SI can be attained in realistic models of the solar nebula have yet to be established.

In this work, we ask whether the conditions under which the SI can produce gravitationally bound particle overdensities can actually be met in the first million years of evolution in globally turbulent PPDs.

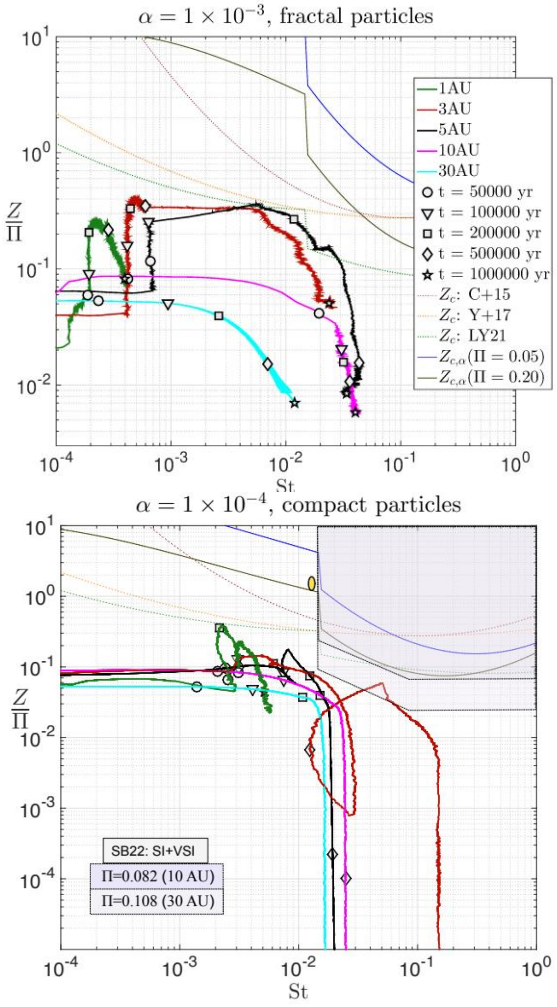

Figure 1. Temporal trajectories over 1 Myr in Z/Π – St parameter space for turbulent growth models with fractal aggregates ($\alpha = 10^{-3}$) and compact particles ($\alpha = 10^{-4}$) plotted for selected disk radial locations as indicated. Selected times are indicated by open symbols. Also shown are the predicted critical curves for Z_c (SI occurrence regions, colored dotted curves) for the laminar case from various studies [15-17], as well as the updated occurrence curve that include an external source of turbulence [17, solid-colored curves] for two characteristic values of Π achieved in our models. Additional regions for VSI turbulence with SI [22] are shown in the shaded regions.

Methods: To explore this question, we analyze previously conducted self-consistent particle growth simulations [20-21] for both fractal aggregates and compact particles in the presence of global turbulence with values of $\alpha = 10^{-4}$ - 10^{-3} thought to characteristic of this epoch in PPDs [5-6]. Our initial disk mass is 0.2 $M_{\odot}$, and initial metallicity is 0.014, and are meant to represent a Class I PPD shortly after the infall stage [see 20]. These simulations span the first Myr which provided a long enough baseline such that the likelihood of strong and efficient acting SI to arise is moving in the direction of less probability. As input, we use the time series generated during each simulation that track the change (temporal trajectories) of the relevant properties, namely the local metallicity *Z*, the mass-dominant particle or aggregate Stokes number St, and the background normalized pressure gradient Π, across the disk. We then compare these to the SI occurrence boundary extension of [17] envisioned to apply to a globally (isotropic) turbulent PPD, and additionally to the predicted SI occurrence boundary predicted by [22] based on their simulations of the VSI (Vertical Shear Instability anisotropic turbulence).

Results: In Figure 1, we plot the temporal trajectories in *Z*/Π – St parameter space of a model for fractal growth (top panel, with $\alpha = 10^{-3}$), and for compact particle growth (bottom panel, with $\alpha = 10^{-4}$) over 1 Myr (selected times indicated by open symbols) at 1, 3, 5, 10, and 30 au. The dotted colored curves correspond to the laminar SI occurrence boundaries of [15-17], while the solid-colored curves correspond to the extended turbulent condition of [17] for two values of Π that envelope characteristic values obtained in our simulations. The shaded regions in the $\alpha = 10^{-4}$ case corresponds to the condition derived by [22] for simulations with SI and VSI, for Π values at 10 and 30 au (the simulations of [22] are for distances ≥ 10 au).

For our selected models we find quite generally that within the first Myr of evolution that there are no times where the temporal trajectories cross the SI occurrence boundaries. Values of St and *Z* change due to growth, drift and fragmentation as well as disk cooling and evolving evaporation fronts which account for the wayward trajectories. The main reason for this is that as growth proceeds to larger St, particles are subject to drift and the local *Z* concurrently decreases sharply to small values, veering trajectories away from the SI occurrence regions. Figure 2 further illustrates that the result is the same at all other radial locations and for two additional models (see caption). We acknowledge that this does not preclude that SI may operate at much later times when the disk is significantly evolved (Class II, e.g., via photoevaporation), and/or in very cold, low mass disks.

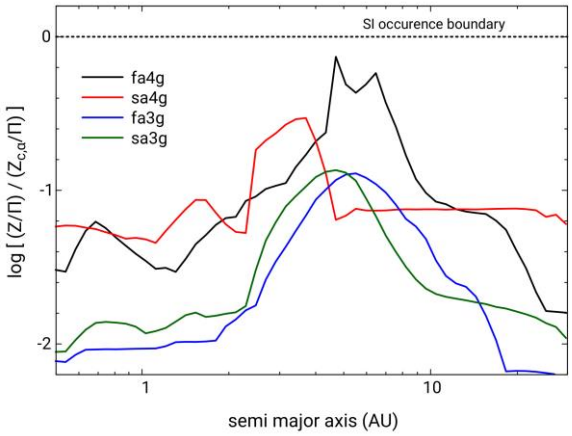

Figure 2. Maximum value for *Z*/Π from our models achieved over 1 Myr for models from Fig. 1, plus two additional models for fractal ($\alpha = 10^{-4}$) and compact growth ($\alpha = 10^{-3}$). These curves are obtained by comparing the evolving St and Π at each radial location and compared with the SI occurrence boundary in the presence of external turbulence of [17] inputting our evolving values of Π. Each radial location reaches its maximum at different times, with a different St associated with them. Plotting in this format makes it easier to visualize that in order to breach the SI occurrence boundary, the ratio of our evolving *Z*/Π to that determined using the condition from [17] must exceed unity, which does not occur for any of the models considered.

References: [1] Kruijer, T. S. et al. (2017) *PNAS, 112,* 6712–6716. [2] Segura-Cox, D. M. et al. (2020) *Nature*, *586*, 228. [3] Krot, A. N. et al. (2009) *GeoCoA, 73*, 4963. [4] Simon, J. I. et al. (2019) *ApJL, 884*, L29. [5] Teague, R. et al. (2016), *A&A, 592,* A49. [6] Flaherty, K. M. et al. (2017). *ApJ, 843*, 131. [7] Lyra, W. and Umurhan, O. M. (2019), *PASP, 131*, 072001. [8] Lesur et al. (2022), *arXiv e-prints*, arXiv:2203.09821. [9] Birnstiel et al. (2010), *A&A, 513*, A79. [10] Estrada, P. R. et al. (2016), *ApJ, 818*, 200. [11] Morbidelli, A. et al. (2009), *Icarus, 204*, 558. [12] Youdin, A. N. and Goodman, J. (2005), *ApJ, 620*, 459. [13] Drążkowska, J. et al. (2016), *A&A, 594*, A105. [14] Carrera, D., et al. (2017), *ApJ, 839,* 16. [15] Carrera, D. et al. (2015), *A&A, 579*, A43. [16] Yang, C.-C. Et al. (2017), *A&A, 606*, A80. [17] Li, R. and Youdin, A. N. (2021), *ApJ, 919*, 107. [18] Umurhan, O. M. et al. (2020), *ApJ, 895*, 4. [19] Chen, K. and Lin, M.-K. (2021), *ApJ, 891,* 132. [20] Estrada, P. R. et al. (2022), *ApJ, 936,* 42. [21] Estrada. P. R. and Cuzzi, J. N. (2022), *ApJ, 936*, 40. [22] Schäfer, U. and Johansen, A. (2022), *A&A, 666,* A98.